DEM-based stress transmission in asphalt mixture skeleton filling system

Xing, Chao; Liu, Bo; Sun, Zhiqi; Tan, Yiqiu; Liu, Xueyan; Zhou, Changhong

Important note
To cite this publication, please use the final published version (if applicable).
Please check the document version above.

DEM-based stress transmission in asphalt mixture skeleton filling system

Chao Xing [a], Bo Liu [b], Zhiqi Sun [c,*], Yiqiu Tan [d], Xueyan Liu [e], Changhong Zhou [f]

[a] School of Transportation Science and Engineering, Harbin Institute of Technology, No. 73, Huanghe Road, Nangang District, Harbin, Heilongjiang, China
[b] School of Transportation Science and Engineering, Harbin Institute of Technology, No. 73, Huanghe Road, Nangang District, Harbin, Heilongjiang, China
[c] State Key Laboratory of Mechanical Behavior and System Safety of Traffic Engineering Structures, Shijiazhuang Tiedao University, No. 17, North 2nd Ring Road (East), Changan District, Shijiazhuang, Hebei, China
[d] School of Transportation Science and Engineering, Harbin Institute of Technology, No. 73, Huanghe Road, Nangang District, Harbin, Heilongjiang, China
[e] Section of Road Engineering, Faculty of Civil Engineering & Geosciences, Delft University of Technology, Stevinweg 1, 2628 CN Delft, The Netherlands
[f] School of Architecture and Transportation Engineering, Guilin University of Electronic Technology, No. 1, Jinji Road, Qixing District, Guilin, Guangxi, China

ARTICLE INFO	ABSTRACT
Keywords: Asphalt mixtures Mesostructure DEM Skeleton filling system Contact force transmission	Asphalt mixture is a skeleton filling system consisting of aggregate, asphalt, and mineral powder. High performance asphalt mixture design is directly affected by internal stress transmission of skeleton filling system. In this paper, the discrete element method based on digital image was employed to study the stress transmission. By analyzing the effect of skeleton structure on the contact force between aggregate and mortar, it is concluded that the skeleton aggregate in the asphalt mixture is the main stress transmission medium. The lower the degree of disruption, the higher the contact force of skeleton aggregate. At the same time, the variation coefficient of contact force of asphalt mortar with low filling coefficient is larger and the localization phenomenon is more serious. By analyzing the effect of mortar properties on the contact force between aggregate and mortar, it is concluded that the lower the modulus of asphalt mortar, the higher the degree of localization of contact force and the more likely to have local damage.

1. Introduction

Asphalt mixture is made up of aggregates that are stacked together and the interlocking between the aggregates maintains the stability of the asphalt mixture [1,2]. At the same time, asphalt mixture is composed of aggregates of different sizes, and the transfer of forces between aggregates has a great influence on the performance of asphalt mixes. Studies have shown that the aggregates can be divided into skeleton aggregates, disruption aggregates and filling aggregates, the so-called skeleton-filling system, and their proportions directly affect the resistance to deformation [3]. The internal force transfer characteristics are the key to reveal the effect of skeleton-filling system on mechanical properties. Stress measurement devices are difficult to measure the internal force contact and therefore to explain the complex damage behavior of asphalt mixtures. Therefore, it is necessary to use numerical simulation methods to obtain the internal meso-mechanical response of asphalt mixtures.

The Discrete Element Method (DEM) can simulate the force transfer process between aggregates during damage. Modeling with DEM includes the following three main methods:

(1) Asphalt mixture is simulated by ideal equal or unequal diameter spheres. Collop [4,5] modeled cylindrical asphalt mixture specimens with equal diameter spheres and simulated compressive creep tests. Abbas [6] modeled columnar asphalt mortar specimens by simulating equal diameter spheres of asphalt and filler. Cai [7] and Chen [8] modeled different sizes of aggregates by non-equal diameter spheres and established axial compression cylindrical specimens and penetration test specimens respectively.

(2) Digital images allow extraction of aggregate and mortar locations in asphalt mixtures, and fill the aggregate and mortar locations with equal diameter balls. Many researchers [9–15] developed image-based cylindrical specimens to simulate compressive strength and dynamic modulus tests. Peng [16] and Mahmoud [17] established image-based indirect tensile test specimens of asphalt mixtures for strength and mechanical response analysis. Kim [18–20] established an image-based unilateral opening

Table 1
Percentage of aggregates (%) in asphalt mixtures.

Types of mixture	Size of sieve (mm)										
	16	13.2	9.5	4.75	2.36	1.18	0.6	0.3	0.15	0.075	<0.075
AC-16	5.0	11.0	14.0	22.0	14.0	9.5	7.0	5.0	3.0	3.5	6.0
SMA-16	5.0	20.0	20.0	29.0	6.5	1.5	3.0	2.5	1.0	1.5	10.0
OGFC-16	5.0	15.0	22.5	36.5	5.0	4.0	2.5	2.0	2.0	1.5	4.0

fracture test model was developed. Huang [21] suggested an image-based multilayer structural model for asphalt pavements. Xu [22,23] analyzed the temperature effects and meso-mechanical responses of pavement by image-based models.

(3) Asphalt mixtures are simulated by customized polygonal particles that can be agglomerates formed by small spheres or ellipsoids. Wang [24] built cylindrical specimens by simulating aggregates with equivalent ellipsoids. Liu [25] and Yu [26,27] simulated aggregates by randomly releasing small ball clusters and established a cylinder model for micromechanics and modal analysis. Dan [28] provided randomly placed spheres of unequal diameters by indirect tensile specimens, and then simulated aggregates of different shapes by replacing the spheres with clusters.

Since discrete particles are used to simulate the internal structure of materials, DEM is suitable for studying the meso-structural properties of heterogeneous materials. Studies on asphalt mixtures have focused on dynamic modulus, creep properties, fracture properties, and heat conduction. Collop [4,5] used such discrete elements to simulate the creep properties of asphalt mixtures under uniaxial compression and derived the relationship between the bulk elastic modulus and Poisson's ratio. Kim [18–20] obtained the fracture mechanism of heterogeneous materials by discrete element model analysis. You [29,30] predicted the dynamic modulus of asphalt mixtures by 2D and 3D DEMs. Papagiannakis [31] predicted the plastic deformation of asphalt mixture by DEM, and the predicted results were consistent with the results of the Hamburg rutting test. Li [32] performed computer-aided design of asphalt mixtures using discrete elements and obtained the relationship between asphalt dosage and volume parameters by simulating compaction. Huang [21,33] analyzed the thermal effect of asphalt mixture structural layer in laboratory and field through the discrete element thermal analysis model, and the results showed that the discrete element could effectively obtain the temperature field distribution inside the asphalt structural layer.

The existing discrete element numerical simulations of asphalt mixtures mainly aimed at macroscopic problems such as modulus, creep and fracture, and the statistical analysis of local contact forces is insufficient. For skeleton and filling systems, the variation of local contact forces caused by different disruption states is very important to reveal the damage mechanism of asphalt mixtures. Therefore, in this paper, discrete element modeling was carried out based on real images of asphalt mixtures to obtain the transmission law of aggregate contact forces under real aggregate distribution states. The objective of this paper is to obtain the effect of skeleton filling state on the stress transmission of asphalt mixture through the contact force analysis of DEM. The results lay a foundation for the design method of asphalt mixture based on skeleton and filling coefficient.

2. Materials and methods

2.1. Materials and gradations

AC (Asphalt Concrete), SMA (Stone Mastic Asphalt) and OGFC (Open Graded Friction Course) asphalt mixture with a maximum nominal particle size of 16 mm was used in this study. The residual percentages for each sieve are shown in Table 1. If aggregates larger than 1.18 mm

Table 2
Percentage of different materials in asphalt mortar (%).

Type of mixture	0.6	0.3	0.15	0.075	<0.075	asphalt
AC-16	24.0	17.0	10.0	12.0	21.0	16.0
SMA-16	12.0	10.0	4.0	6.0	41.0	26.0
OGFC-16	16.0	13.0	13.0	9.0	25.0	25.0

Table 3
Properties of SBS modified asphalt.

Properties	Unit	Test result	Specification requirements	Specification
Penetration, 25 ℃, 100 g, 5 s	0.1 mm	66.9	60~80	JTG F40
Ductility (5 ℃, 5 cm/min)	cm	43.3	≥30	
Softening point	℃	66.5	≥55	

Table 4
Disruption and filling coefficients of asphalt mixtures.

Gradation Types	Disruption coefficient	Filling coefficient
AC-16	2.05	2.23
SMA-16	0.67	1.21
OGFC-16	1.13	0.83

were removed from the asphalt mixture, the mass percentages of aggregate and asphalt in the asphalt mortar are shown in Table 2. The SBS (Styrene-Butadiene-Styrene) polymer modified asphalt is used in this paper. Base on the test methods of "Standard Test Methods of Bitumen and Bituminous Mixtures for Highway Engineering (JTG E20)", the properties of the asphalt are shown in Table 3. The Properties need to meet requirements of "Technical Specifications for Construction of Highway Asphalt Pavements (JTG F40)".

2.2. Disruption and filling coefficients

To characterize the skeleton-filling system of asphalt mixture, our team calculated the disruption coefficient and filling coefficient in previous research [3]. For asphalt mixtures with a maximum nominal particle size of 16 mm, aggregates smaller than 1.18 mm were defined as filling aggregates and mixed with asphalt to form asphalt mortar. For coarser aggregates, aggregates in the size range of 4.75 mm ~ 1.18 mm are defined as disruption aggregates, while aggregates larger than 4.75 mm are skeleton aggregates [3]. According to the classification method, the disruption and filling coefficients can be calculated, as shown in Table 4.

The disruption coefficient indicates the effect of disruption aggregates on the contact between skeleton aggregates, while the amount of mortar in the asphalt mixture was characterized by the filling coefficient. The results in the table were consistent with our common knowledge that the coarse aggregate skeleton was better in SMA and OGFC asphalt mixture and that more asphalt mortar was present in AC asphalt mixture. In the following study, the disruption and filling coefficients will be used to compare the meso-structure and contact forces.
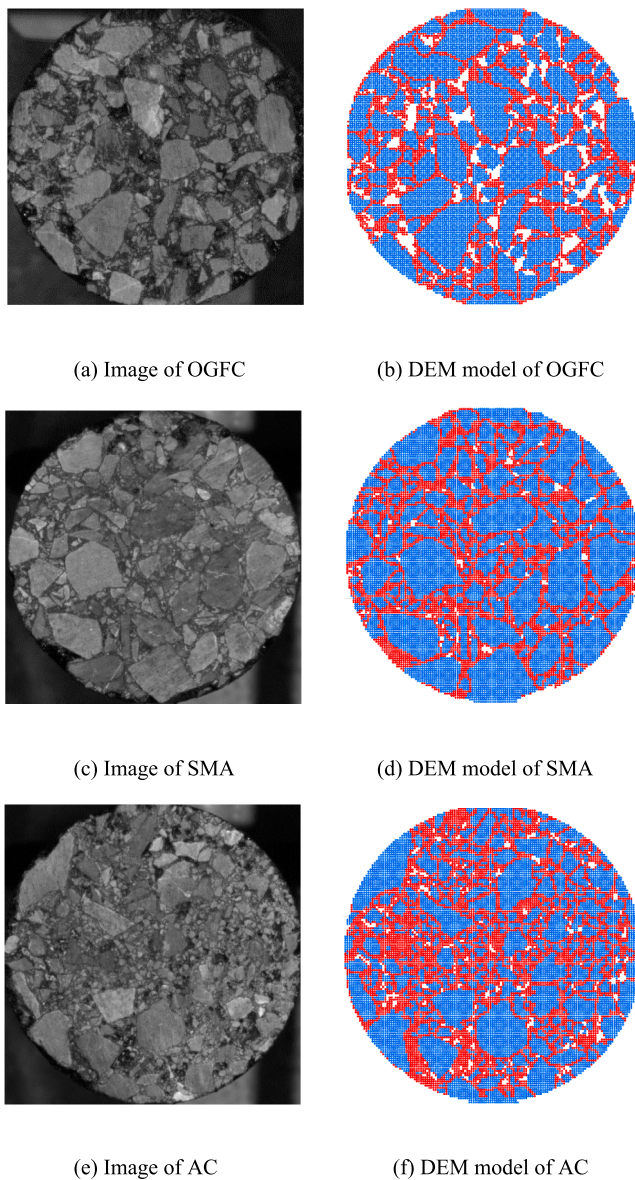
(a) Image of OGFC

(b) DEM model of OGFC

(c) Image of SMA

(d) DEM model of SMA

(e) Image of AC

(f) DEM model of AC

Fig. 1. Image and DEM model of the three types of asphalt mixtures.

3. Modeling and parameter determination

3.1. DEM model

The DEM simulation was performed by PFC software. The digital image processing method allowed to divide the asphalt mixture into aggregates, asphalt mortar and voids. The geometric positions of the aggregates and asphalt mortar were obtained from the images [10,12,15]. The digital image processing method was composed of fuzzy network noise reduction and contrast enhancement, multilevel thresholding, watershed transformation image segmentation. In the PFC2D software, the aggregates were represented by clumps, while the mortar was simulated by ball element. The images of the asphalt mixtures were shown in Fig. 1(a)–(e), and the DEM model was created in Fig. 1(b)–(f).

3.2. Modelling parameters of asphalt mortar and aggregate

Aggregates and asphalt mortars belong to the categories of elasticity and viscoelasticity, respectively. The viscoelastic parameters of asphalt mortar were obtained by DSR (Dynamic Shear Rheometer) frequency scan tests. The test temperatures in this study included 10 ℃, 20 ℃, 30
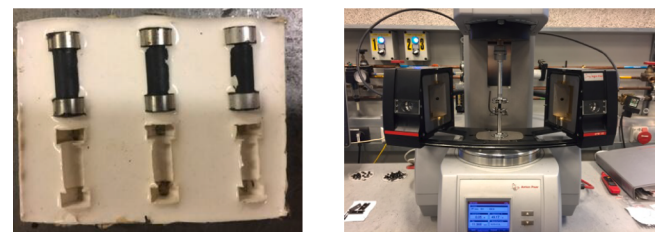
(a) Prepared asphalt mortar sample   (b) DSR equipment

Fig. 2. Test samples and DSR equipment.

℃, 40 ℃, 50 ℃ and 60 ℃, and the frequency range was 0.01 Hz ~ 50 Hz. The height and diameter of the column are 10 mm and 6 mm. The test samples and DSR equipment are shown in Fig. 2.

According to the time–temperature equivalence principle, the complex modulus curves at different temperatures can be transformed into a wide frequency domain complex modulus curve at the same temperature, which is the complex modulus master curve. According to the time–temperature equivalence principle and Christensen Anderson Marasteanu (CAM) model, the complex modulus master curves of three asphalt mortars at 20 °C were obtained by the programming solution method.

The Burgers model was used to describe the viscoelastic properties of the asphalt mortar. The complex modulus and phase angle of the asphalt mortar can be obtained by DSR test, and the main curve of the complex modulus and phase angle obtained by experiment can be fitted by Burgers model. The main curve and Burges fitting curve of the three asphalt mortars are shown in Fig. 3.

As shown in Fig. 3, for these three asphalt mortars, the Burgers model was able to fit the main curve of the composite modulus well. By fitting, the Burgers model parameters of the three asphalt mortars can be obtained, as shown in Table 5. According to the conversion relationship between Burgers macro model parameters and micro model parameters [13], the elasticity parameters and viscosity parameters of the three asphalt mortars are shown in Tables 6 and 7.

The modulus of elasticity of aggregates is much larger than that of mortar, and the variation with temperature is very small. According to the results of related literature [9,18–20], the elastic modulus of aggregate is 55.5 Gpa, and the Poisson's ratio of basalt stone is about 0.23 ~ 0.32. The Poisson's ratio of the aggregate used in this research is 0.25. Therefore, the shear modulus of aggregate is 22.2 Gpa. According to the macro–micro parameter transformation relationship of aggregates, the aggregate stiffness and contact stiffness of aggregates are shown in Table 7.

Assuming that the modulus of elasticity of steel is 200 Gpa and Poisson's ratio is 0.25, the steel particle stiffness parameters and the aggregate-steel contact stiffness parameters are shown in Table 8. Given the modulus of elasticity and shear modulus of the aggregate and the microscopic Burgers parameters of the mortar, the microscopic parameters of the Burgers contact model between the aggregate and mortar can be calculated and the calculation results are shown in Tables 9 and 10.

4. Results and discussion

Based on the DEM model of the asphalt mixture developed above and the determined model parameters, this section analyzes the effect of meso-structure and properties of the asphalt mortar on the internal mechanical response of the asphalt mixture. The contact forces between the aggregate and the mortar are utilized to illustrate the effect of the skeleton filling state on the mechanical responses of the asphalt mixture.
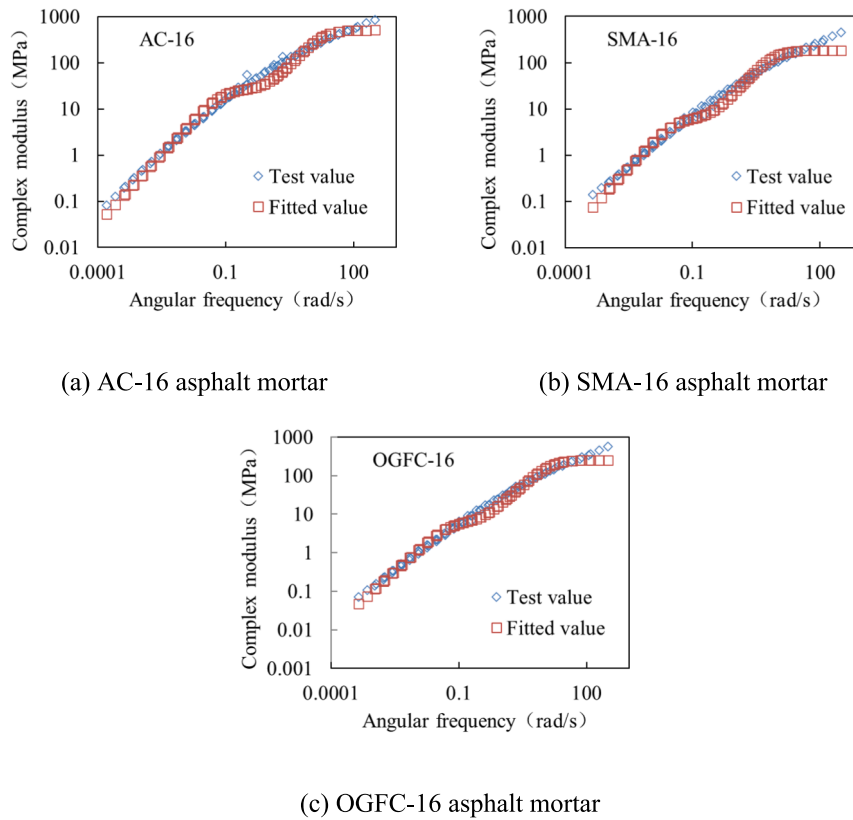
(a) AC-16 asphalt mortar

(b) SMA-16 asphalt mortar

(c) OGFC-16 asphalt mortar

Fig. 3. Complex modulus and Burgers model fitting curve.

Table 5
Burgers macro model parameter.

Mortar type	E_1 (MPa)	E_2 (MPa)	η_1 (MPa ·s)	η_2 (MPa ·s)
AC-16	508.5	30.2	325.8	32.2
SMA-16	184.4	7.4	171.4	27.2
OGFC-16	253.9	7.8	106.0	22.4

Table 6
Burgers model micro elastic parameter of asphalt mortar.

Mortar type	K_{mn} (MPa·m)	K_{ms} (MPa·m)	K_{kn} (MPa·m)	K_{ks} (MPa·m)
AC-16	508.5	169.5	30.2	10.1
SMA-16	184.4	61.5	7.4	2.5
OGFC-16	253.9	84.6	7.8	2.6

Table 7
Burgers model micro viscous parameter of asphalt mortar.

Mortar type	C_{mn} (MPa·m·s)	C_{ms} (MPa·m·s)	C_{kn} (MPa·m·s)	C_{ks} (MPa·m·s)
AC-16	325.8	108.6	32.2	10.7
SMA-16	171.4	57.1	27.2	9.1
OGFC-16	106.0	35.3	22.4	7.5

Table 8
Micro stiffness parameters of aggregate.

k_n (GPa)	k_s (GPa)	K_n (GPa)	K_s (GPa)
111.0	44.4	55.5	22.2

Table 9
Micro stiffness parameters of aggregate-steel.

k_n (GPa)	k_s (GPa)	K_n (GPa)	K_s (GPa)
400.0	160.0	86.9	34.8

Table 10
Burgers model micro elastic parameter of asphalt mortar-aggregate.

Mortar type	K_{mn} (MPa·m)	K_{ms} (MPa·m)	K_{kn} (MPa·m)	K_{ks} (MPa·m)
AC-16	1007.8	336.4	60.5	20.2
SMA-16	367.6	122.6	14.7	4.9
OGFC-16	505.6	168.6	15.7	5.2

4.1. Influence of meso-structure on contact force of aggregates

In this paper, the indirect tensile test was used for the mechanical response, and the loading speed was 50 mm/min. Through the analysis of the DEM calculation results, the mechanical response was relatively stable at 1% vertical strain, so the contact force at 1% vertical strain of the indirect tensile test was chosen for the analysis. The contact force distribution of the aggregates is shown in Fig. 4.

From Fig. 4, it can be seen that for the three types of asphalt mixtures, the load is mainly borne by the coarse aggregates, while the fine aggregates are scattered among the coarse aggregates and bears a smaller load. The diameter of the aggregates can be calculated based on the circular transformation of the equivalent area. The relationship between the equivalent diameter of the aggregate and the contact force is shown in Fig. 5.

As shown in Fig. 5, in general, the contact force increases with the increase of aggregate size. In SMA and OGFC asphalt mixture, some of
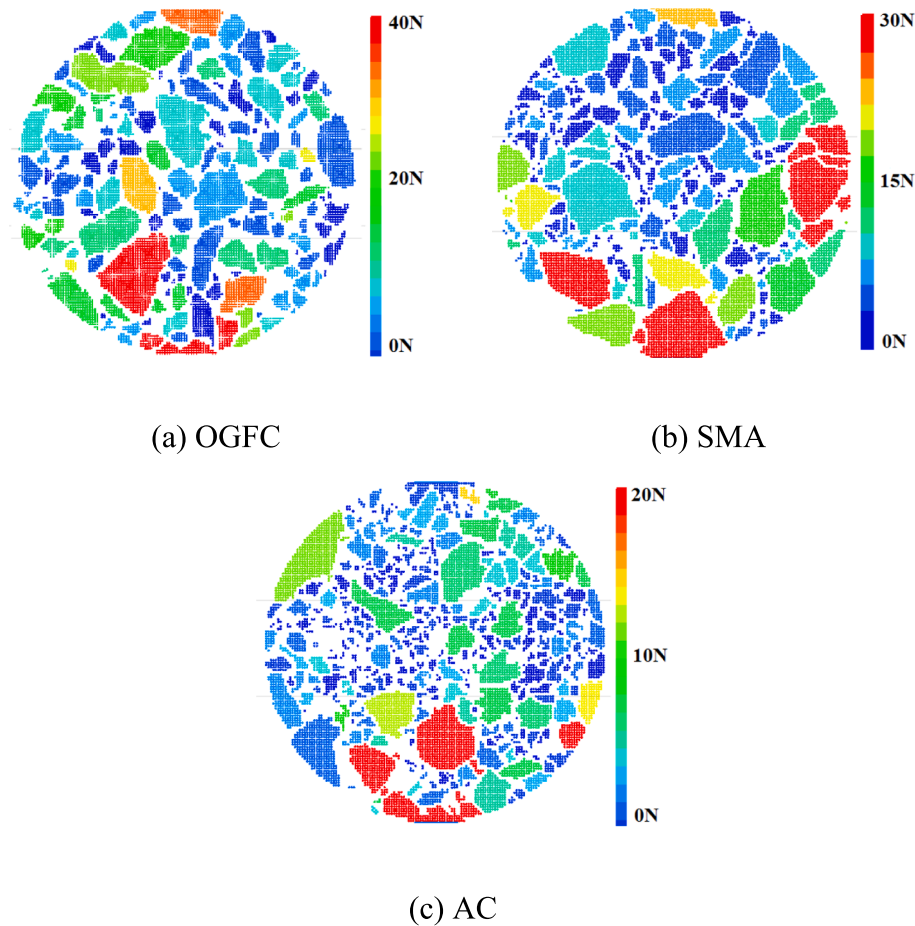
(a) OGFC

(b) SMA

(c) AC

Fig. 4. Relationship between aggregate size and contact force.

the fine aggregates also bear larger contact forces, while in AC asphalt mixture, the contact force distribution of fine aggregates is concentrated in the small force area.

This phenomenon shows that coarse aggregates are generally the main load bearing units of asphalt mixtures in different skeletal states. Part of the fine aggregates in OGFC and SMA asphalt mixtures are located in the contact area between coarse aggregates. They are the transmission medium between coarse aggregates, so they are subjected to higher contact forces. For AC asphalt mixes, the coarse aggregates are suspended among many fine aggregates, and the reasons for the lower contact forces on the fine aggregates include. (1) Some fine aggregates fill the voids between coarse aggregates and bear less contact force. (2) Due to the large number of fine aggregates, the contact force transmission is relatively dispersed, resulting in a smaller contact force for each aggregate.

Based on the data of contact forces and aggregate sizes, the average contact forces of different aggregates for the three asphalt mixtures are shown in Fig. 6.

It can be seen from Fig. 6 that the average contact force tends to increase with the increase of aggregate size. For the 13.2 mm and 16 mm gradations, the average contact force fluctuates slightly due to the small number of aggregates. For different asphalt mixture, the order of the average contact force is OGFC > SMA > AC.

In order to describe the role of skeleton aggregate and disruption aggregate during loading, the average contact force ratio of skeleton aggregate to disruption aggregate was used to evaluate the bearing capacity of the skeleton aggregate. It can be calculated by formula (1). The average contact forces and contact force ratios are shown in Table 11.

$$R = \frac{F_s}{F_d} \tag{1}$$

where R is the contact force ratio, F_s is the average contact forces of skeleton aggregates, F_d is the average contact forces of disruption aggregates.

It can be seen from Table 11 that the average contact force of skeleton aggregates is significantly higher than that of disruption aggregates, which indicates that the skeleton aggregates are the main force transmission medium in asphalt mixture. Meanwhile, the order of contact force ratio of the three asphalt mixtures is SMA > OGFC > AC, which is consistent with the disruption coefficient, indicating that the lower the disruption state is in the asphalt mixtures, the higher the contact force of the skeleton aggregates are.

4.2. Influence of meso-structure on contact force of mortar

The meso-structure not only affects the force transfer of the aggregate, but also the contact force distribution of mortar-aggregate and mortar-mortar. The contact tension and pressure distribution of the mortar in the indirect tensile test are shown in Fig. 7(a), (c) and (e). The green rectangle represents the pressure, the blue rectangle represents the tension, and the wider the rectangle represents the value of the contact force. To clearly observe the local tension and pressure distribution, the red boxes in the center of the specimens are enlarged as shown in Fig. 7(b), (d) and (f).

From Fig. 7, it can be seen that for these three asphalt mixtures, the large contact forces were mainly generated in the middle of the specimen. The contact compression forces for OGFC and SMA asphalt
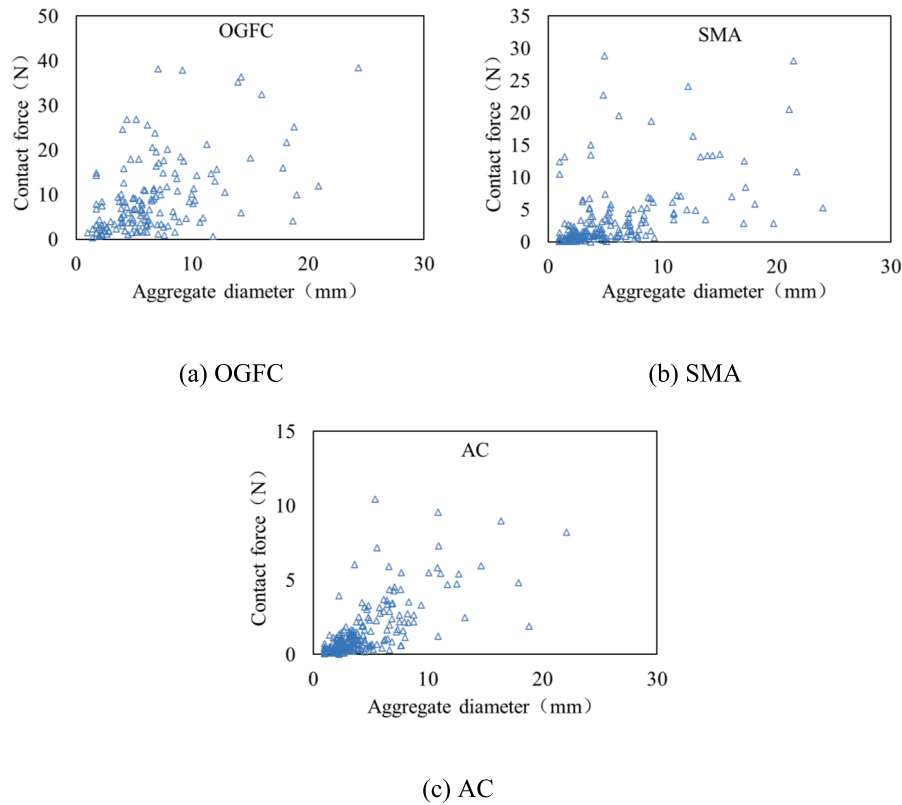
(a) OGFC

(b) SMA

(c) AC

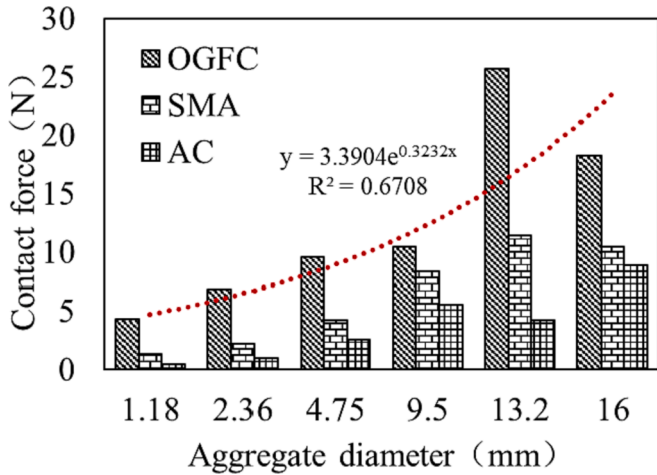**Fig. 5.** Relationship between aggregate size and contact force.

Fig. 6. Average contact forces of aggregates with different size.

Table 11
Burgers model micro viscous parameter of asphalt mortar-aggregate.

Mortar type	C_{mn} (MPa·m·s)	C_{ms} (MPa·m·s)	C_{kn} (MPa·m·s)	C_{ks} (MPa·m·s)
AC-16	651.5	217.2	64.4	21.5
SMA-16	342.7	114.2	54.5	18.2
OGFC-16	212.0	70.7	44.9	15.0

mixtures were concentrated at the contact location of the aggregates. In contrast, the contact compression forces for AC asphalt mixtures were scattered over wider areas, with little difference between different areas. By magnifying local areas, it can be seen that the contact force is mainly

expressed as pressure in the vertical direction and tension in the horizontal direction, which is consistent with the mechanical response of the indirect tensile test.

According to the calculation results of DEM, the contact forces between the mortars can be extracted. The contact tension and pressure distribution between mortar and mortar for the three asphalt mixtures are shown in Fig. 8.

As can be seen from Fig. 8, for all three asphalt mixtures, most of the contact forces are small and the percentage of high contact forces is small.

This indicates that the asphalt mixtures showed localization phenomenon during loading with relatively high local contact forces. Comparing the three asphalt mixtures, OGFC presents a lower percentage of high contact force areas than AC and SMA, and the localization phenomenon is more severe. Similarly, the mortar-aggregate contact tension and pressure can be obtained from the DEM model. The contact force results for the three asphalt mixtures are shown in Fig. 9.

It can be seen from Fig. 9 that the distribution of contact forces for mortar-aggregate is similar to that of mortar-mortar and also shows a strong localization phenomenon. In order to describe the differences in the localization behavior of the three asphalt mixtures, the mean values and coefficients of variation were calculated for tension and pressure, respectively. The coefficient of variation is a dimensionless parameter that indicates the degree of dispersion of the data. Large coefficients of variation indicate severe localization. The results of the mean and coefficient of variation calculations are shown in Tables 12 and 13.

By comparing the average contact forces in Tables 12 and 13, the average contact tension force is greater than the average contact pressure, and the mortar-aggregate contact force is greater than the mortar-mortar contact force. This indicates that in the indirect tensile test, the mortar was subjected to higher tensile forces, which led to tensile damage of the mortar. At the same time, the interface between the aggregate and mortar was more susceptible to larger contact forces, which led to interface damage. The contact force relationship between
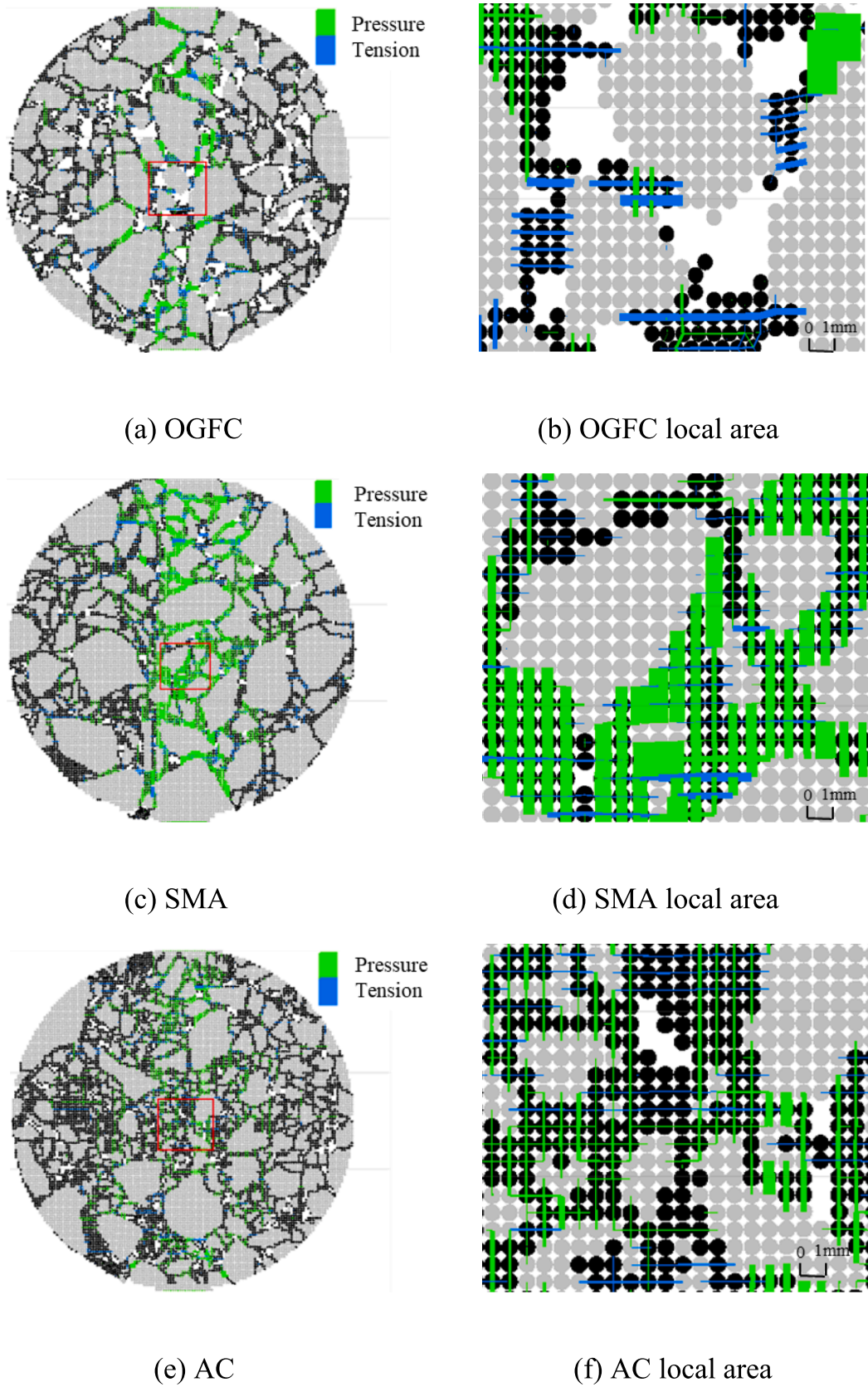
(a) OGFC

(b) OGFC local area

(c) SMA

(d) SMA local area

(e) AC

(f) AC local area

Fig. 7. Contact force distribution of mortar.

(a) OGFC contact tension

(b) OGFC contact pressure

(c) SMA contact tension

(d) SMA contact pressure

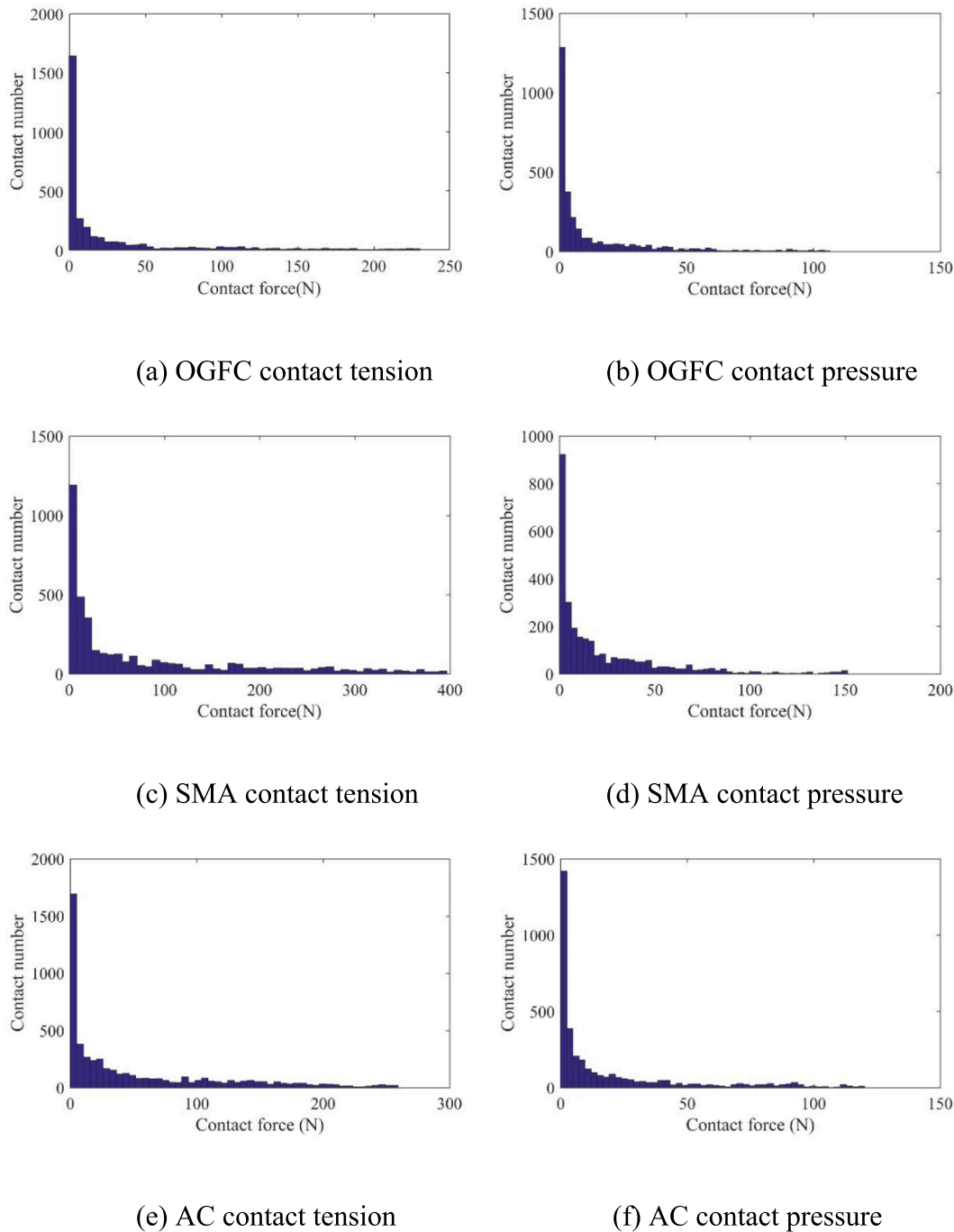(e) AC contact tension

(f) AC contact pressure

Fig. 8. Distribution of contact force in asphalt mortar.

the three asphalt mixtures was SMA > AC > OGFC. The reason for this phenomenon was that the number of aggregates of OGFC was low and the contact force was high, as shown in Fig. 8(a) and (b), resulting in a low average contact force. While the high contact force area of SMA and AC is larger, the contact force concentration of SMA is more serious, resulting in a larger overall contact force value.

By comparing the coefficient of variation of contact force, the order of the coefficient of variation of the three asphalt mixtures is OGFC > SMA > AC, indicating that the coefficient of variation of contact force is larger for asphalt mortar with lower filling coefficient. The reason for the above phenomenon is that the asphalt mixture with lower filling coefficient, the filling area of the mortar is smaller, and it is easier to produce local high contact force during the loading process, and the

localization phenomenon is more serious.

4.3. Influence of asphalt mortar properties on contact force of aggregates

The transmission characteristics of the contact forces between the aggregate and the mortar in asphalt mixtures are influenced not only by the mesoscopic structure, but also by the mechanical properties of the asphalt mortar. This section focuses on the effect of mechanical properties of asphalt mortar on the contact forces inside the asphalt mixture. According to the performance of AC-16 mortar, the elastic and viscous model parameters of Burgers were increased and decreased by 20%, respectively, and the aggregate properties were kept constant. The macro-Burgers model parameters of asphalt mortar were used in this
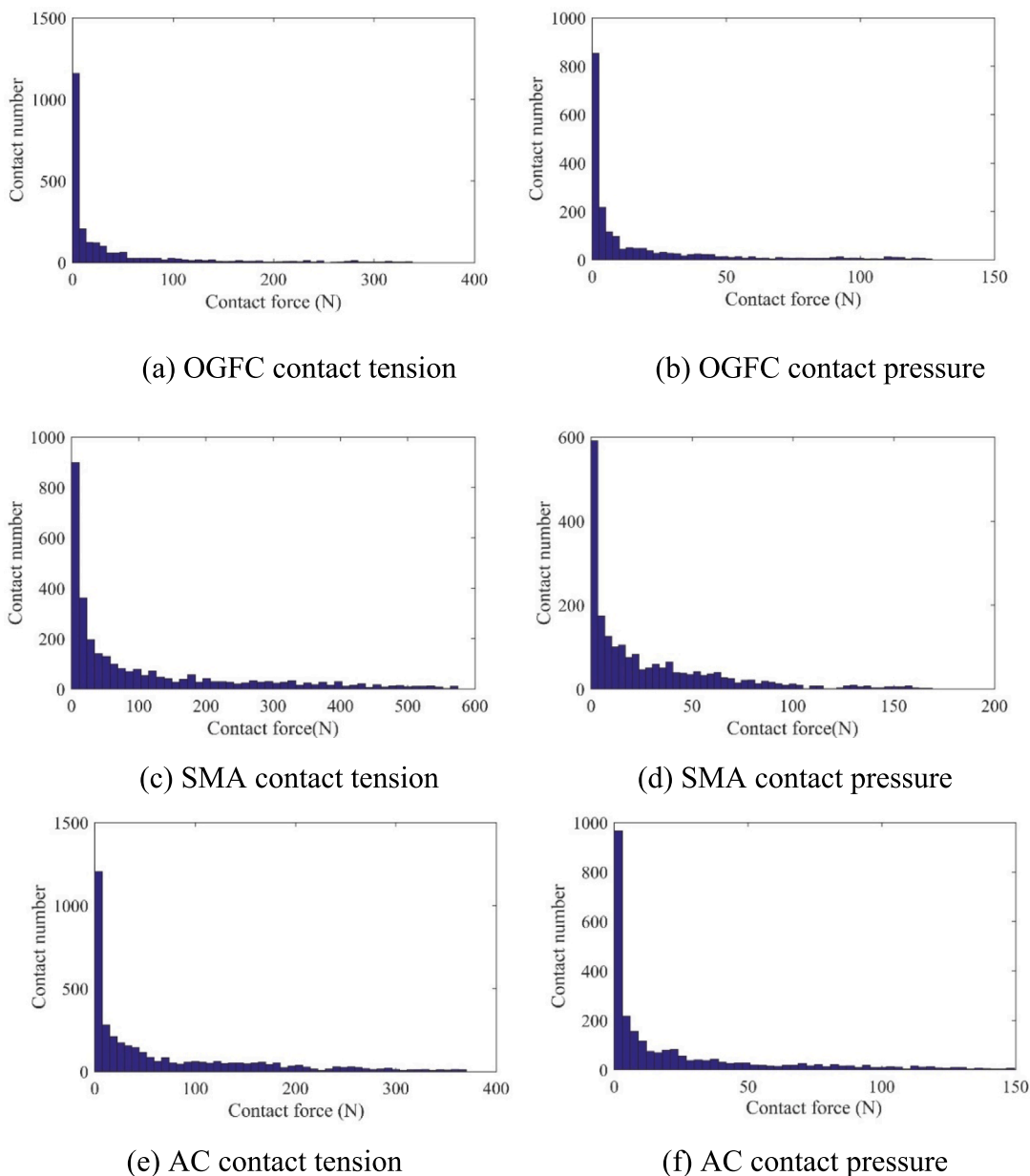
(a) OGFC contact tension

(b) OGFC contact pressure

(c) SMA contact tension

(d) SMA contact pressure

(e) AC contact tension

(f) AC contact pressure

Fig. 9. Distribution of contact force between asphalt mortar and aggregate.

Table 12
Contact force of skeleton and disruption aggregates.

Mixture type	Average contact forces of skeleton aggregates (N)	Average contact forces of disruption aggregates (N)	Contact force ratios
OGFC	11.08	4.88	2.27
SMA	5.96	1.79	3.33
AC	2.33	1.51	1.54

section, as shown in Table 14.

The parameters of the asphalt mortar model in Table 14 were input into the discrete element model, and the parameters of the three asphalt mixture models with reduced modulus and 20% increased mortar load were obtained for aggregate contact force, mortar contact force and mortar-aggregate interface contact force for three different mortar properties of asphalt mixture aggregate contact force as shown in Fig. 10.

It can be seen from Fig. 10 that when the elastic and viscoelastic properties of the mortar are increased or decreased, the contact force of

Table 13
Mean value and variable coefficient of mortar-aggregate contact force.

Indexes	OGFC tension	SMA tension	AC tension	OGFC pressure	SMA pressure	AC pressure
Mean(N)	35.97	106.31	69.70	17.76	28.58	23.15
Variation coefficient (%)	177.5	129.1	125.2	159.5	141.0	111.2

Table 14
Mean value and variable coefficient of mortar-mortar contact force.

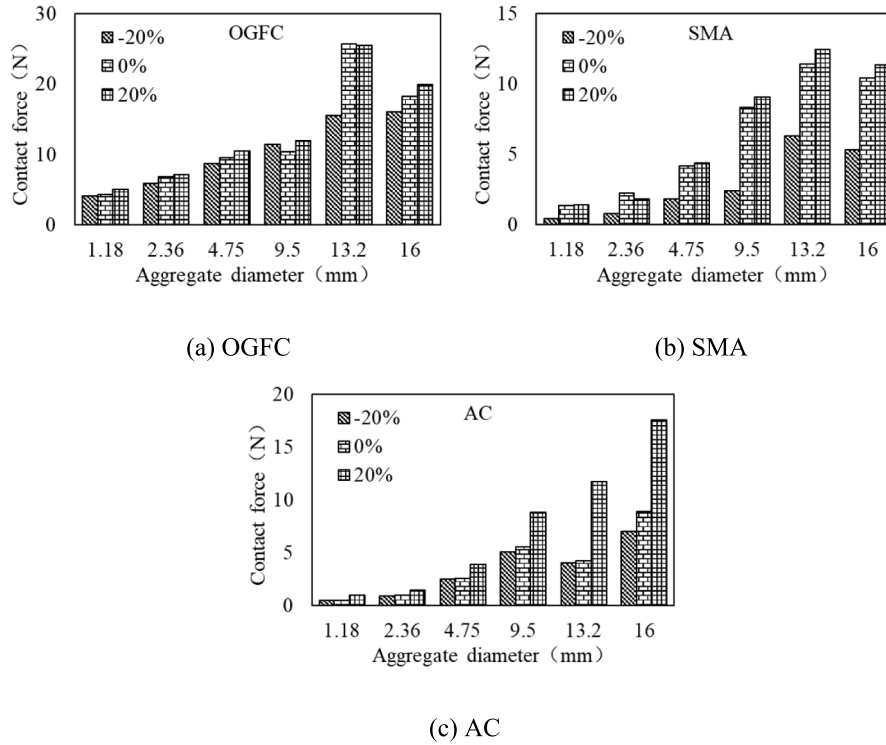| Indexes	OGFC tension	SMA tension	AC tension	OGFC pressure	SMA pressure	AC pressure
Mean value (N)	25.88	81.44	51.30	13.17	21.99	18.14
Variation coefficient (%)	181.1	126.7	124.4	160.4	145.2	125.3

(a) OGFC   (b) SMA

(c) AC

Fig. 10. Relationship between aggregate size and contact force.

Table 15
Burgers macro model parameter of asphalt mortar.

Mortar type	E_1/MPa	E_2/ MPa	η_1/ MPa ·s	η_2/ MPa ·s
Mortar (−20%)	406.80	24.16	260.64	25.76
Mortar (0)	508.50	30.20	325.80	32.20
Mortar (+20%)	610.20	36.24	390.96	38.64

the aggregates with different aggregate sizes also increases with the increase in aggregate sizes. It indicates that for different mortar properties, the aggregate with large aggregate size is the main load bearing unit of asphalt mixture, and the relationship between aggregate size and contact force does not change with the change of mortar modulus. Meanwhile, it can be found that the contact force of aggregates increases with the increase of mortar modulus. The main reason is that the internal contact force of the high modulus material is larger when the same deformation is applied to the material in the displacement loading mode. The average contact forces of the skeleton aggregates and disruption aggregates were calculated and the statistical results are shown in Table 15.

It is clear from Table 15 that the contact force of the skeleton aggregates is higher than that of the disruption aggregates. Meanwhile, increasing the modulus of mortar can improve the contact force of both skeleton aggregates and disruption aggregates. As for the contact force of skeleton aggregates and disruption aggregates, the load-bearing effect of both types of aggregates is of more interest with the change of mortar modulus. The contact force ratio (contact force of skeleton aggregates/
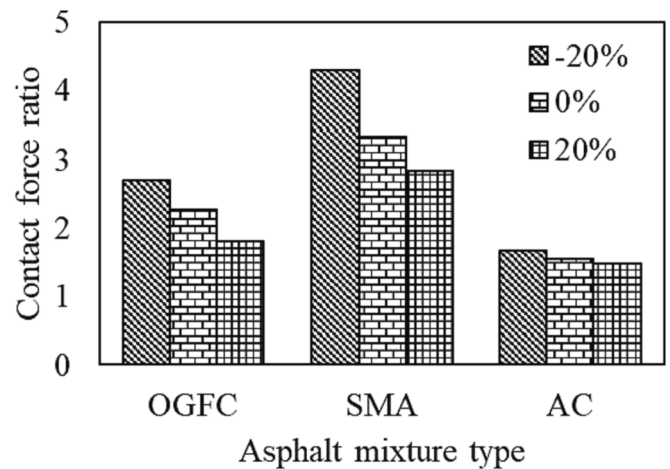

Fig. 11. Relationship between contact force rate and asphalt mortar property.

contact force of disruption aggregates) can reflect the changing relationship of the load bearing effects of the two types of aggregates. The contact forces of different mortar properties are shown in Fig. 11.

It can be seen from Fig. 11 that the increase or decrease of mortar modulus does not change the contact force ratio relationship of the three asphalt mixtures, and the rule is also SMA > OGFC > AC. It is also found that the contact force ratio is decreasing with the increase of asphalt

Table 16
Contact force of skeleton and disruption aggregates.

Grain Type	OGFC −20%	OGFC 0%	OGFC 20%	SMA −20%	SMA 0%	SMA 20%	AC −20%	AC 0%	AC 20%
Skeleton aggregates	9.96	11.08	17.10	2.63	5.96	7.07	1.85	2.33	3.95
Disruption aggregates	3.69	4.88	9.50	0.61	1.79	2.50	1.11	1.51	2.65

(a) Mortar-aggregate
contact tension force

(b) Mortar-mortar
contact tension force

(c) Mortar-aggregate
contact compression force

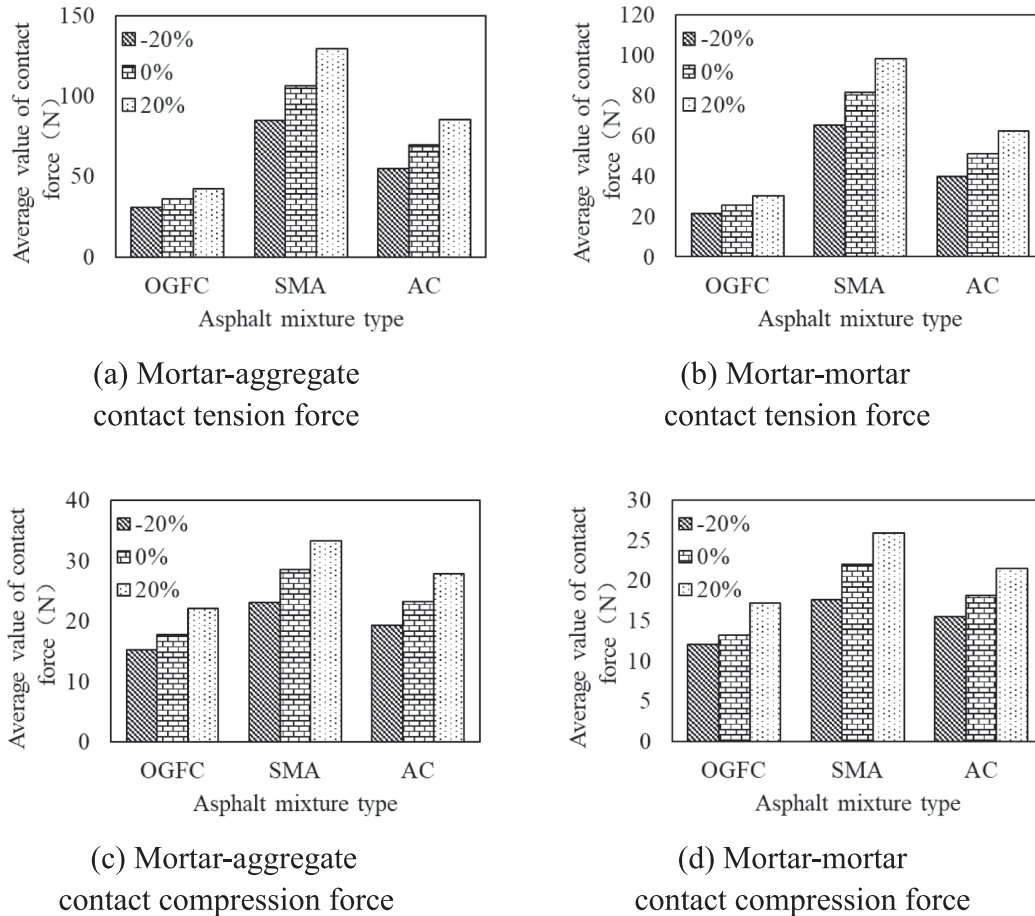(d) Mortar-mortar
contact compression force

Fig. 12. Relationship between contact force and asphalt mortar property.

mortar modulus, which indicates that the lower the mortar modulus, the higher the contact force of the skeleton aggregates and the more obvious the bearing effect. The reason for the above phenomenon is that the lower the mortar modulus is, the less the disruption aggregates and mortar support the skeleton aggregates, so the skeleton aggregates are subjected to a higher contact force than the disruption aggregates (see Table 16).

4.4. Influence of asphalt mortar properties on contact force of mortar

Through the calculation results of different mortar performance models, the average contact tension of mortar-mortar and mortar-aggregate can be extracted, and the variation law of the average contact force with the mortar modulus is shown in Fig. 12.

It can be seen from Fig. 12 that for different mixture types, different contact types and tensile pressure types, the average contact force tends to increase with the increase in mortar modulus. The reason for this phenomenon is the same as the increase in aggregate contact force. This is because the increase in the material modulus leads to an increase in the contact force within the material under the same deformation conditions. Mortar properties affect not only the load bearing capacity of the

skeleton aggregates, but also the localization behavior of the mortar contact forces. As mentioned above, the localization behavior of mortar contact forces can be expressed by the coefficient of variation of contact forces. The relationship between the coefficient of variation of mortar contact force and mortar properties is shown in Fig. 13.

By comparing the contact tensile forces in Fig. 13(a) and (b), it can be seen that OGFC has the largest coefficient of variation for the different mortar properties, while SMA is slightly larger than AC. By comparing the contact compression forces in Fig. 13(c) and (d), it can be seen that OGFC has the largest coefficient of variation for different mortar properties, while SMA is larger than AC. This indicates that the variation of mortar properties does not affect the relationship between the local degree of contact forces of the three asphalt mixtures, while the local phenomenon is most severe for OGFC asphalt mixture. More notably, it can be found from Fig. 13 that the coefficient of variation of contact force decreases with the increase of mortar modulus parameter for different contact types, different mixture types and contact tensile pressures. It indicates that the lower the asphalt mortar modulus is, the larger the coefficient of variation of contact force is, and the higher the localization of contact force is, the more likely local damage will occur.
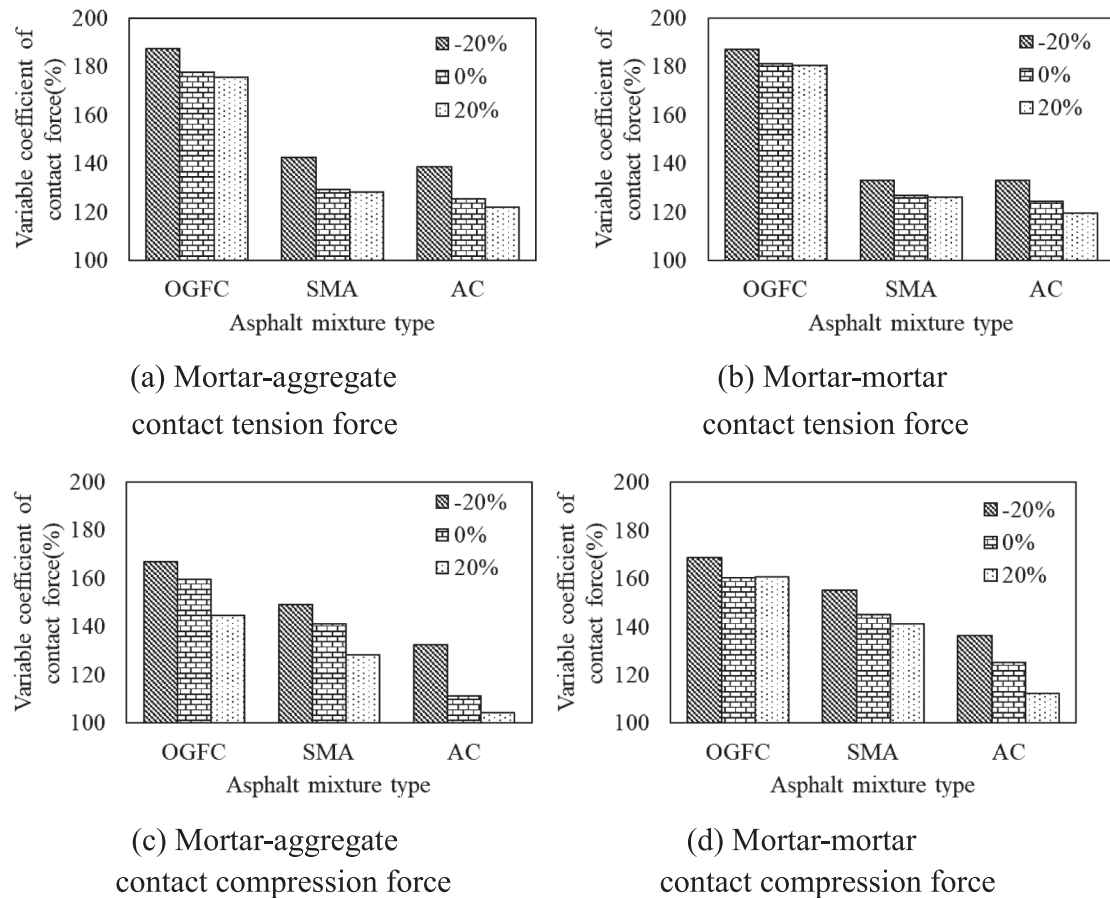
(a) Mortar-aggregate
contact tension force

(b) Mortar-mortar
contact tension force

(c) Mortar-aggregate
contact compression force

(d) Mortar-mortar
contact compression force

Fig. 13. Relationship between contact force variable coefficient and asphalt mortar property.

5. Conclusions

In this paper, a discrete element model of the asphalt mixture was established using DEM and digital image processing techniques, and then the indirect tensile test of the asphalt mixture was simulated. On this basis, the effects of skeleton structure on the meso-mechanical response of the asphalt mixture were analyzed separately, and the main conclusions are as follows.

(1) By analyzing the effect of meso-structure on aggregate contact force, the average value of contact force increases with the increase of aggregate size, and the average value of contact force of skeleton aggregates is significantly higher than that of disruption aggregate. This indicates that skeleton aggregates are the main force transmission medium in asphalt mixture.

(2) By analyzing the effect of meso-structure on the contact force of mortar, it was concluded that the contact compression force of OGFC-16 and SMA-16 asphalt mixtures was concentrated at the contact position of aggregates, and the distribution area of AC asphalt mixtures was more dispersed. For the contact compression force and tensile force, the order of the variation coefficient is OGFC-16 > SMA-16 > AC-16, which indicates that the asphalt mortar with low filling coefficient, the greater the variation coefficient of contact force, the more serious the localization phenomenon.

(3) Analysis from the effect of mortar properties on aggregate contact force. And with the increase of asphalt mortar modulus, the contact force ratio shows a decreasing trend, indicating that the lower the mortar modulus is, the higher the contact force of the skeleton aggregates is, and the more obvious the bearing effect is.

(4) The analysis of the effect of mortar properties on mortar contact force shows that the coefficient of variation of mortar contact force decreases with the increase of mortar modulus parameters, indicating that the lower the modulus of asphalt mortar, the higher the degree of localization of contact force and the more likely local damage occurs.

CRediT authorship contribution statement

Chao Xing: Conceptualization, Methodology, Software, Writing – original draft. **Bo Liu:** Data curation, Writing – original draft. **Zhiqi Sun:** Visualization, Investigation, Writing – review & editing. **Yiqiu Tan:** Supervision. **Xueyan Liu:** Software, Validation. **Changhong Zhou:** Writing – review & editing.

Declaration of Competing Interest

The authors declare that they have no known competing financial interests or personal relationships that could have appeared to influence the work reported in this paper.

Data availability

No data was used for the research described in the article.

References

[1] Y. Tan, Z. Liang, H. Xu, C. Xing, Research on rutting deformation monitoring method based on intelligent aggregate, IEEE Trans. Intell. Transp. Syst. (2022).

[2] Y. Tan, Z. Liang, H. Xu, C. Xing, Internal deformation monitoring of granular material using intelligent aggregate, Autom. Constr. 139 (2022), 104265.

[3] C. Xing, Z. Liang, Y. Tan, et al., Skeleton filling system evaluation method of asphalt mixture based on compressible packing model, Journal of Transportation Engineering, Part B: Pavements 147 (4) (2021) 04021062.

[4] A.C. Collop, G.R. McDowell, Y.W. Lee, Use of the distinct element method to model the deformation behavior of an idealized asphalt mixture, Int. J. Pavement Eng. 5 (1) (2004) 1–7.

[5] A.C. Collop, G.R. McDowell, Y.W. Lee, Modelling dilation in an idealised asphalt mixture using discrete element modelling, Granular Matter 8 (3) (2006) 175–184.

[6] A. Abbas, E. Masad, T. Papagiannakis, A. Shenoy, Modelling asphalt mastic stiffness using discrete element analysis and micromechanics-based models, Int. J. Pavement Eng. 6 (2) (2005) 137–146.

[7] W. Cai, G.R. McDowell, G.D. Airey, Discrete element visco-elastic modelling of a realistic graded asphalt mixture, Soils Found. 54 (1) (2014) 12–22.

[8] J. Chen, H. Li, L. Wang, J. Wu, X. Huang, Micromechanical characteristics of aggregate particles in asphalt mixtures, Constr. Build. Mater. 91 (2015) 80–85.

[9] Z. You, S. Adhikari, Q. Dai, Three-dimensional discrete element models for asphalt mixtures, J. Eng. Mech. 134 (12) (2008) 1053–1063.

[10] Z. You, W.G. Buttlar, Discrete element modeling to predict the modulus of asphalt concrete mixtures, J. Mater. Civ. Eng. 16 (2) (2004) 140–146.

[11] Q. Dai, Z. You, Prediction of creep stiffness of asphalt mixture with micromechanical finite-element and discrete-element models, J. Eng. Mech. 133 (2) (2007) 163–173.

[12] A. Abbas, E. Masad, T. Papagiannakis, T. Harman, Micromechanical modeling of the viscoelastic behavior of asphalt mixtures using the discrete-element method, Int. J. Geomech. 7 (2) (2007) 131–139.

[13] Y. Liu, Q. Dai, Z. You, Viscoelastic model for discrete element simulation of asphalt mixtures, J. Eng. Mech. 135 (4) (2009) 324–333.

[14] S. Adhikari, Z. You, Investigating the sensitivity of aggregate size within sand mastic by modeling the microstructure of an asphalt mixture, J. Mater. Civ. Eng. 23 (5) (2010) 580–586.

[15] M.J. Khattak, A. Khattab, H.R. Rizvi, S. Das, M.R. Bhuyan, Imaged-based discrete element modeling of hot mix asphalt mixtures, Mater. Struct. 48 (8) (2015) 2417–2430.

[16] Y. Peng, Y. Wan, L.J. Sun, Three-dimensional discrete element modelling of influence factors of indirect tensile strength of asphalt mixtures, Int. J. Pavement Eng. (2017) 1–10.

[17] E. Mahmoud, E. Masad, S. Nazarian, Discrete element analysis of the influences of aggregate properties and internal structure on fracture in asphalt mixtures, J. Mater. Civ. Eng. 22 (1) (2009) 10–20.

[18] H. Kim, W.G. Buttlar, Multi-scale fracture modeling of asphalt composite structures, Compos. Sci. Technol. 69 (15) (2009) 2716–2723.

[19] H. Kim, M.P. Wagoner, W.G. Buttlar, Micromechanical fracture modeling of asphalt concrete using a single-edge notched beam test, Mater. Struct. 42 (5) (2009) 677–689.

[20] H. Kim, W.G. Buttlar, Discrete fracture modeling of asphalt concrete, Int. J. Solids Struct. 46 (13) (2009) 2593–2604.

[21] K. Huang, T. Xu, G. Li, R. Jiang, Heating effects of asphalt pavement during hot in-place recycling using DEM, Constr. Build. Mater. 115 (2016) 62–69.

[22] J. Xu, N. Li, T. Xu, Temperature changes of interlaminar bonding layer in different seasons and effects on mechanical properties of asphalt pavement, Int. J. Pavement Res. Technol. 15 (3) (2022) 589–605.

[23] J. Xu, C. Kong, T. Xu, Displacemental and mesomechanical responses of semi-flexible pavement based on discrete element method, Int. J. Pavement Res. Technol. 3 (2021) 1–14.

[24] L. Wang, J.Y. Park, Y. Fu, Representation of real particles for DEM simulation using X-ray tomography, Constr. Build. Mater. 21 (2) (2007) 338–346.

[25] Y. Liu, Z. You, Visualization and simulation of asphalt concrete with randomly generated three-dimensional models, J. Comput. Civil Eng. 23 (6) (2009) 340–347.

[26] H. Yu, S. Shen, Impact of aggregate packing on dynamic modulus of hot mix asphalt mixtures using three-dimensional discrete element method, Constr. Build. Mater. 26 (1) (2012) 302–309.

[27] H. Yu, S. Shen, A micromechanical based three-dimensional DEM approach to characterize the complex modulus of asphalt mixtures, Constr. Build. Mater. 38 (2013) 1089–1096.

[28] H.C. Dan, Z. Zhang, J.Q. Chen, H. Wang, Numerical simulation of an indirect tensile test for asphalt mixtures using discrete element method software, J. Mater. Civ. Eng. 30 (5) (2018) 04018067.

[29] Z. You, S. Adhikari, M.E. Kutay, Dynamic modulus simulation of the asphalt concrete using the X-ray computed tomography images, Mater. Struct. 42 (5) (2009) 617–630.

[30] S. Adhikari, Z. You, 3D Discrete element models of the hollow cylindrical asphalt concrete specimens subject to the internal pressure, Int. J. Pavement Eng. 11 (5) (2010) 429–439.

[31] A.T. Papagiannakis, H.M. Zelelew, E. Mahmoud, Simulation of asphalt concrete plastic deformation behavior, J. Mater. Civ. Eng. 30 (3) (2018) 04018025.

[32] Y. Li, L. Wang, Computer-aided procedure for determination of asphalt content in asphalt mixture using discrete element method, Int. J. Pavement Eng. 18 (9) (2017) 765–774.

[33] K. Huang, T. Xu, G. Li, R. Jiang, The feasibility of DEM to analyze the temperature field of asphalt mixture, Constr. Build. Mater. 106 (2016) 529–559.